Journal of Proteomics 187 (2018) 161–170

Contents lists available at ScienceDirect

Journal of Proteomics

journal homepage: www.elsevier.com/locate/jprot

SWATH-MS quantitative proteomic investigation of nitrogen starvation in Arabidopsis reveals new aspects of plant nitrogen stress responses

Fu-Yuan Zhu[a,b,1], Mo-Xian Chen[c,1], Wai-Lung Chan[b], Feng Yang[b], Yuan Tian[c], Tao Song[c], Li-Juan Xie[d], Ying Zhou[d], Shi Xiao[d], Jianhua Zhang[c,e,*], Clive Lo[b,**]

[a] Co-Innovation Center for Sustainable Forestry in Southern China, College of Biology and the Environment, Nanjing Forestry University, Nanjing, China
[b] School of Biological Sciences, The University of Hong Kong, Pokfulam Road, Hong Kong, China
[c] Shenzhen Research Institute, The Chinese University of Hong Kong, Shenzhen, China
[d] State Key Laboratory of Biocontrol and Guangdong Provincial Key Laboratory of Plant Resources, School of Life Sciences, Sun Yat-sen University, Guangzhou, China
[e] Department of Biology, Hong Kong Baptist University, and State Key Laboratory of Agrobiotechnology, The Chinese University of Hong Kong, Shatin, Hong Kong, China

ARTICLE INFO

Keywords:
SWATH-MS
Arabidopsis
Nitrogen stress response
Phospholipid
14-3-3

ABSTRACT

Nitrogen is an essential macronutrient for plant growth and crop productivity. The aim of this work was to further investigate the molecular events during plant adaptation to nitrogen stress. Here, we present a SWATH-MS (Sequential window acquisition of all theoretical mass spectra)-based quantitative approach to detect proteome changes in Arabidopsis seedlings following nitrogen starvation. In total, 736 proteins of diverse functions were determined to show significant abundance changes between nitrogen-supplied and nitrogen-starved Arabidopsis seedlings. Functional categorization revealed the involvement of nitrogen stress-responsive proteins in biological processes including amino acid and protein metabolism, photosynthesis, lipid metabolism and glucosinolate metabolism. Subsequent phospholipid profiling of Arabidopsis seedlings showed changes in phospholipid composition that may enhance membrane fluidity as a response to nitrogen starvation. Moreover, an Arabidopsis *grf6* T-DNA insertion mutant was found to have a nitrogen stress-sensitive phenotype. GRF6 is a 14-3-3 protein with elevated abundance upon nitrogen starvation and it may function as a positive regulator during nitrogen stress adaptation.

1. Significance

Low nitrogen use efficiency in crop plants leads to economically inefficient cropping systems while excessive nitrogen fertilization continuously causes environment problems. Here, we describe the proteome changes in Arabidopsis seedlings following nitrogen starvation, highlighting several metabolic processes. A potential positive regulatory role of a 14-3-3 protein (GRF6) was also revealed. Our work provides new insights into plant nitrogen stress responses at the proteome level, potentially useful for dissecting the molecular components of nitrogen responses in plants for adapting to low nitrogen availability.

2. Introduction

Nitrogen nutrition is an important factor essential for plant growth and productivity [1], influencing many biological processes in plants such as flowering, senescence and photosynthesis [2]. Nitrogen sources can be available from organic and inorganic compounds in the soil. Amino acids are the main organic sources whereas nitrate and ammonium are the predominant inorganic sources [3, 4]. Crop growth is often limited by low bio-availability of nitrogen in the soil which needs to be supplemented with extra nitrogen fertilizers during the farming season. However, due to the low nitrogen use efficiency of crop plants, excessive applications of nitrogen fertilizer result in deleterious environmental problems including eutrophication and soil pollution [5, 6]. Better understanding of nitrogen nutrition and stress responses in plants is needed for developing strategies to enhance nitrogen use efficiency, hence reducing excessive fertilizer usages.

Nitrogen use efficiency primarily depends on nitrogen uptake efficiency, which is mediated by plasma membrane-localized influx

* Corresponding author at: Department of Biology, Hong Kong Baptist University, and State Key Laboratory of Agrobiotechnology, The Chinese University of Hong Kong, Shatin, Hong Kong, China.
** Corresponding author at: School of Biological Sciences, The University of Hong Kong, Pokfulam Road, Hong Kong, China
E-mail addresses: jzhang@hkbu.edu.hk (J. Zhang), clivelo@hku.hk (C. Lo).
[1] These authors contributed equally to this work.

https://doi.org/10.1016/j.jprot.2018.07.014
Received 7 February 2018; Received in revised form 4 July 2018; Accepted 19 July 2018
Available online 23 July 2018
1874-3919/

transporters [7, 8]. There are different mechanisms in plants for the uptake of ammonium and nitrate which are the main nitrogen sources in soils. For ammonium uptake, six ammonium transporters belonging to the AMT/MEP/Rh (AMT) superfamily in Arabidopsis have been demonstrated to have high affinity for ammonium [9, 10]. Five of the six Arabidopsis *AtAMT* genes showed root expression which was up-regulated during low nitrogen availability [9]. Under such condition, about 90% of the high affinity ammonium uptake is contributed by AtAMT1;1, AtAMT1;2 and AtAMT1;3 addictively [9, 11]. AtAMT1.1, AtAMT1.3 and AtAMT1.5 are responsible for absorbing ammonium directly from the soil, whereas AtAMT1.2 transports apoplastic ammonium into the cell [9, 11]. For nitrate uptake, the NITRATE TRANSPORTER 1/PEPTIDE TRANSPORTER family (NPF) and NITRATE TRANSPORTER 2 (NRT2) family have been identified in Arabidopsis [12]. NRT2 members are high-affinity nitrate transporters accounting for 95% of the uptake capacity, whereas the NPF members showed a low affinity for nitrate [13], suggesting that NRT2 transporters are critical for efficient nitrate uptake to sustain growth under low nitrogen availability. Furthermore, nitrate flux studies revealed that AtNRT2.1, AtNRT2.2, AtNRT2.4 and AtNRT2.5 are the predominant contributors for nitrate transport. According to their spatial expression patterns during nitrogen deficiency, AtNRT2.4 and AtNRT2.5 are involved in nitrate uptake from soil while AtNRT2.1 plays a role in apoplastic nitrate absorption [14]. Interestingly, AtNRT1.1 has been demonstrated with the dual roles of affinity transport and nitrate-sensing [15].

Transcriptomic and proteomics analyses of plants during nitrogen deficiency have been conducted to provide insights on the regulatory mechanisms of nitrogen utilization and stress responses [16, 17]. So far, knowledge on the regulatory mechanisms of plant nitrogen response at protein levels remains limited due to the small number of identified proteins from these studies. In the present work, changes in the proteome profile in Arabidopsis seedlings under nitrogen deprivation were examined using the SWATH-MS (sequential windowed acquisition of all theoretical mass spectra) approach which provides quantification of protein abundances and large-scale identification of nitrogen stress-responsive proteins. A total of 1676 proteins were quantitatively identified in Arabidopsis seedlings, 736 of which were found to be differentially expressed upon nitrogen starvation (cut-off: z-value ≥ 2.0 or $\leq$-2.0 at $P < 0.05$). The nitrogen stress-responsive proteins have been categorized into different biological processes including amino acid biosynthesis, protein translation, lipid metabolism and glucosinolate metabolism. Phospholipid profiling revealed composition changes in membrane lipid which may enhance fluidity upon nitrogen deficiency. Finally, mutant analysis revealed a potential positive regulatory role for a 14-3-3 protein (GRF6) with increased abundances in nitrogen-starved Arabidopsis seedlings.

3. Results and discussion

To ensure a meaningful nitrogen deficiency treatment for proteomic analyses, several physiological parameters after nitrogen deprivation were first determined. Seven-day-old Arabidopsis seedlings were cultured on 2 mL of either MS or MS medium without nitrogen sources (MS-N) for 48 h. As shown in Fig. 1, nitrogen starvation caused reduction of ammonium, nitrate, protein, and chlorophyll contents in the seedlings. Subsequently, a SWATH-MS-based proteomics investigation was performed to investigate the effects of nitrogen starvation on proteome changes in Arabidopsis seedlings. After combining the data from four biological replicates, a total of 1676 unique proteins were quantified by MarkerView (information of the identified peptides and proteins is shown in Table S1). Proteins with a z-value of above 2.0 or below -2.0 ($P < 0.05$) were considered as nitrogen stress-responsive in this study. As such, a total of 736 proteins were found to show significant abundance changes upon nitrogen starvation: 312 increased and 424 decreased (Table S2).

To examine the potential coordinately regulated proteins contributing to nitrogen-starvation responses, functional classification of the nitrogen stress-responsive proteins was performed using the MapMANBIN system (http://ppdb.tc.cornell.edu/dbsearch/searchacc.aspx) (Table S2). Proteins with significantly increased or decreased abundance changes were assigned to 27 functional categories. Accordingly, proteins belonging to the categories “Protein metabolism”, “Amino acid metabolism” and “Photosynthesis” constitute the largest groups of nitrogen stress-responsive proteins, suggesting that these processes were substantially affected during the nitrogen deficiency. For proteins with increased abundances, “Protein metabolism”, “Signaling, and “Transport” constituted the top 3 functional categories (Fig. 2A). For proteins with decreased abundances, “Protein metabolism”, “Photosynthesis”, and “Amino acid metabolism” constituted the top 3 functional categories (Fig. 2B). These findings suggested that different biological processes were activated or repressed in Arabidopsis seedlings to cope with nitrogen starvation.

3.1. Impact on amino acid biosynthesis and protein translation

KEGG classification of the nitrogen stress-responsive proteins provides a quick overview on the metabolic pathways that are most influenced in the nitrogen-starved Arabidopsis seedlings. We identified 44 enzymes that could be mapped to different amino acid biosynthesis pathways, most of them showing reduced protein abundances (Fig. 3). It is well known that the amino acids glutamine, asparagine and aspartate are important nitrogen carriers in plants generated by the assimilation of inorganic nitrogen [3]. Therefore, nitrogen deprivation would block the incorporation of nitrogen into amino acids, leading to an overall down-regulation of amino acid biosynthesis. A similar phenomenon was observed in barley and wheat during nitrogen starvation [18, 19]. Meanwhile, several proteins associated with amino acid degradation showed increased abundances upon nitrogen starvation (Table S2), presumably representing a feedback response to generate endogenous nitrogen sources.

Limitation of nitrogen supply is also expected to impact protein synthesis. Consistently, 93 proteins involved in translation were found to have reduced abundances, including a large number of ribosomal proteins in cytosol and plastids as well as several initiation and elongation factors (Table S3). This would indicate an overall down-regulation of protein synthesis, consistent with the lower protein content in the nitrogen-starved Arabidopsis seedlings (Fig. 1A). On the contrary, 19 proteins participating in translation showed elevated abundances upon nitrogen starvation (Table S3). Presumably they are involved in the synthesis of proteins specific for nitrogen stress responses. Interestingly, two of the translation initiation factors, eIF4A (At3G19760) and eIF4E (At4G18040), are associated with abiotic and biotic stresses, respectively [20, 21]. *eIF4A* expression is induced following cold or heat treatment and gene disruption resulted in increased sensitivities to both cold and heat stresses [20, 21]. On the other hand, eIF4E and its isoform eIF(iso)4E are indispensable for potyvirus infection and gene disruption led to resistance [22, 23]. In fact, several translation initiation factors were considered as potential targets for genetic manipulation to improve plant performance and adaptation [20, 21]. Hence, the roles of translation initiators like eIF4A and eIF4E in nitrogen starvation responses may be further elucidated for potential applications.

3.2. Impact on photosynthesis: light reactions and carbon dioxide assimilation

Nitrogen deficiency inhibits photosynthesis through reduction of chlorophyll content and suppression of ribulose bisphosphate carboxylase/oxygenase (Rubisco) enzymatic activities [24, 25]. In this study, a total of 29 photosynthesis-related proteins were detected with altered abundances: 22 decreased and 7 increased (Table S2). Those proteins with reduced abundances are essential components of photosynthetic

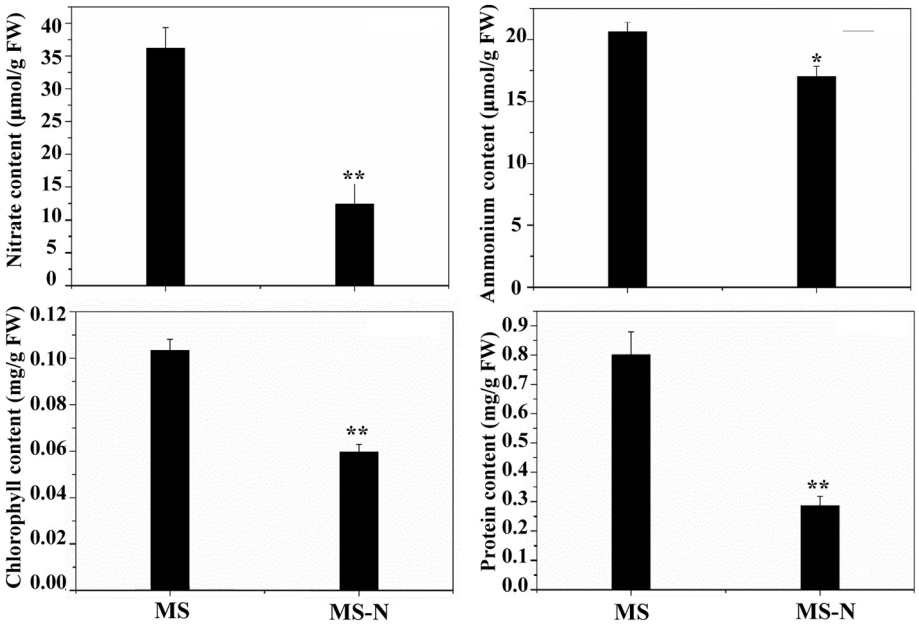

Fig. 1. Changes in ammonium, nitrate, chlorophyll and proteins contents in Arabidopsis WT seedlings upon nitrogen starvation. Arabidopsis seeds were germinated on MS agar plates. After 7 days, seedlings were transferred to MS or MS-N liquid medium and grown for 48 h. Error bars represent SE ($n = 5$); *P < 0.05; **P < 0.01 by Student's *t*-test. FW, fresh weight.

enzyme complexes including photosystem I and II (PSI and *Psi*I), photosynthetic electron transport, F-type ATP synthase and the light-harvesting chlorophyll protein complex (Fig. 4A), indicating that the light reactions were strongly impaired upon nitrogen starvation. Similarly, CO_2 assimilation appeared to be suppressed with reduced abundances of Calvin cycle enzymes, including Rubisco proteins (ATCG00490, AT5G38420, AT5G38430 and AT1G67090) required for CO_2 fixation, phosphoglycerate kinases (AT3G12780 and AT1G56190) and glyceraldehyde-3-phosphate dehydrogenase (At1G42970) involved in the reduction stage; Ribulose-5-phosphate-3-epimerase (AT5G61410), and phosphoribulokinase (AT1G32060) participating in the regeneration of ribulose bisphosphate (Fig. 4B). The overall down-regulation of photosynthetic activities may allow the maintenance of C/N ratio during nitrogen deficiency.

3.3. Impact on lipid metabolism and phospholipid composition

Lipids are essential structural components in cell membranes and energy sources for cellular metabolism. They have recently received considerable attention as important mediators in different biological processes, especially responses to biotic and abiotic stresses [26, 27]. Alteration in carbon chain length and saturation levels in fatty acids could occur in plants in response to environmental cues [28]. In our study, several enzymes with significant abundance changes could be mapped to different reactions in fatty acid biosynthesis (Fig. 5A). Fatty acids are synthesized from acetyl-CoA which undergoes ATP-dependent carboxylation to form malonyl-CoA, followed by the generation of malonyl-ACP [29]. The enzymes involved in these initial reactions were reduced in abundances upon nitrogen starvation, including components of the acetyl-CoA carboxylase complex (At5G16390, At5G35360, AtCG00500) and malonyl-CoA: ACP transacylase (At2G30200). Using acetyl-CoA and malonyl-ACP, the fatty acid synthase (FAS) complex catalyzes repeated cycles of condensation, reduction, dehydration and reduction for the acyl chain elongation. In nitrogen-starved Arabidopsis seedlings, elevated abundances were detected for the FAS components 3-ketoacyl synthase III (AT1G62640) and 3-hydroxyacyl-ACP dehydratase (At2G22230) which are involved in condensation and dehydration, respectively.

Subsequently, we investigated the membrane lipid profiles of Arabidopsis seedlings upon nitrogen starvation by automated electrospray ionization-tandem mass spectrometry (ESI-MS/MS). Overall, there were no significant changes in the levels of total phospholipids, including major species like monogalactosyldiacylglycerol and digalactosyldiacylglycerol, probably due to the opposing abundance changes for different enzymes in fatty acid synthesis. However, the proportions of phosphatidylserine (PS) and phosphatidylethanolamine (PE) in nitrogen-starved seedlings decreased significantly whereas the proportion of phosphatidylcholine (PC) increased significantly (Fig. 5B). Accordingly, the PC/PE ratio is increased by approximately 45% in the nitrogen-starved seedlings. Alteration in the membrane fluidity has been suggested to be a primary signal in stress sensing [30, 31]. In fact, PC can increase membrane fluidity whereas PE can reduce membrane fluidity in plants [32, 33]. Hence, the elevated PC/PE ratio in Arabidopsis seedlings upon nitrogen deprivation (Fig. 5B) may enhance membrane fluidity for nutrient absorption or trigger signals for the activation of downstream events involved in stress adaption.

3.4. Impact on glucosinolate metabolism

Glucosinolates (GSLs) are secondary metabolites mainly found in the *Brassicaceae* family [34]. The glucosinolate biosynthetic pathway includes amino acid chain elongation accompanied by the addition of methyl groups, core structure formation, and secondary modifications of the amino acid chains [34, 35]. As shown in Fig. 6, a number of enzymes involved in the three stages of glucosinolate biosynthesis, including branched-chain aminotransferase 3 (AT3G49680) and 4 (AT3G19710), methylthioalkylmalate synthase 1 (AT5G23010), isopropylmalate isomerase large subunit (AT4G13430), CYP83A1 (AT4G13770), glutathione S-transferase TAU20 (AT1G78370), and GSL hydroxylase (AT2G25450), were detected with decreased abundances in Arabidopsis seedlings following nitrogen deprivation. In contrast, Arabidopsis plants were reported to show enhanced glucosinolate accumulation under ammonium nutrition [36]. Apparently, the levels of glucosinolates are highly correlated with nitrogen availability in Arabidopsis.

Furthermore, glucosinolates could be enzymatically degraded by myrosinases such as beta-thioglucoside glucohydrolases (TGG1 and TGG2) during environmental stress [37], releasing useful byproducts including nitriles, epithionitriles and thiocyanates (Fig. 6). These compounds play an important role in defense against pathogen attack [38] and serve as a nutrient sink to help plants cope with nutrient deficiencies [36, 39]. In fact, TGG1 (AT5G26000) abundance was

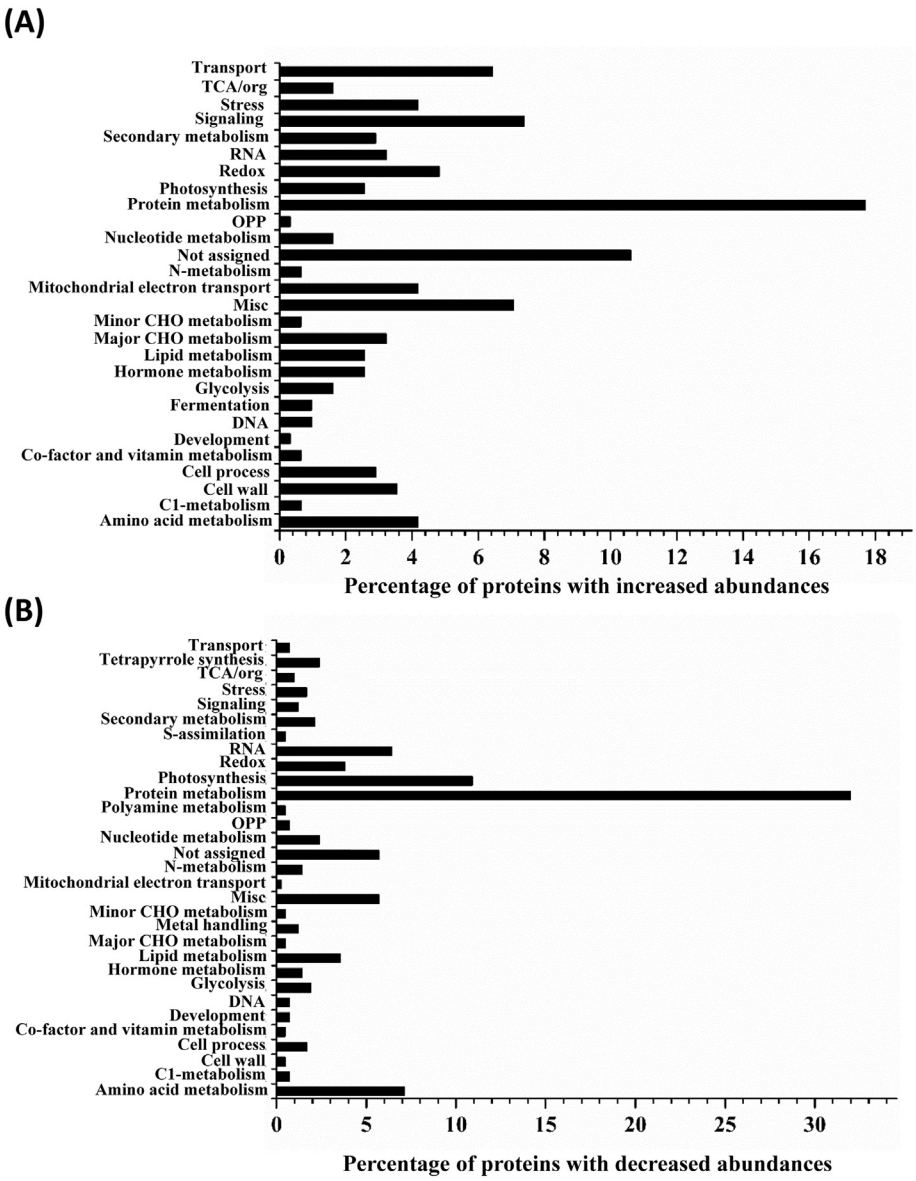

Fig. 2. Functional categorization of nitrogen stress-responsive proteins by the MapMAN BIN system. The plots reveal the involvement of nitrogen stress-responsive proteins in different functional categories showing increased and decreased protein abundances in Arabidopsis seedlings upon nitrogen starvation.

elevated in nitrogen-starved Arabidopsis seedlings. Hence, glucosinolate degradation may be promoted to assist in primary metabolism such as protein synthesis.

3.5. Involvement of the 14-3-3 protein GRF6 as a potential positive regulator of nitrogen stress response

Several 14-3-3 proteins, including the general regulatory factors GRF5 (AT5G16050), GRF6 (AT5G10450), GRF7 (AT3G02520), GRF8 (AT5G65430), and GRF9 (AT2G42590), were elevated in abundances in Arabidopsis seedlings upon nitrogen deprivation. The 14-3-3 proteins have been shown to inhibit NADH: nitrate reductase activity through binding of a phosphorylated motif while they stimulate cytosolic glutamine synthetase 1 (GS1) activity [40, 41]. In this study, we detected reduced abundances of nitrate and nitrite reductases (AT1G37130 and AT2G15620) and elevated abundance of GS1 in nitrogen-starved Arabidopsis seedlings (Fig. 7A). These results implicated a potential regulatory role of 14-3-3 proteins on enzymes involved in nitrogen metabolism (Fig. 7A). We subsequently investigated the involvement of 14-3-3 proteins during nitrogen stress responses using two independent Arabidopsis *grf6* T-DNA mutants. As shown in Fig. 7B, *GRF6* expression was strongly induced in Arabidopsis wild-type (WT) seedlings upon nitrogen starvation. In addition, the *grf6* mutants were more sensitive to nitrogen starvation-induced root inhibition than WT plants (Fig. 7C), suggesting a positive regulatory role of GRF6 in nitrogen stress responses.

Previously,the Arabidopsis 14-3-3 protein GRF6 was reported to be a regulator of abiotic and biotic stress responses. For example, overexpression of GRF6 in cotton resulted in the “stay-green” phenotype and enhanced drought tolerance [42]. In Arabidopsis, the RPW8.2-mediated powdery mildew resistance is dependent on GRF6 which interacts with the C-terminal domain of RPW8.2 [43]. The mechanistic roles of GRF6 in salt and freezing responses have been further elucidated recently. For example, the vacuolar two-pore potassium channel 1 (TPK1) is activated as a salt stress adaption in Arabidopsis. Such activation requires the interaction of TPK1 with GRF6 following the phosphorylation of the 14–3-3 binding motif in TPK1 by calcium-dependent protein kinases [44]. On the other hand, GRF6 functions as a negative regulator of freezing tolerance in Arabidopsis. After phosphorylation by the cold-responsive plasma membrane protein kinase 1,

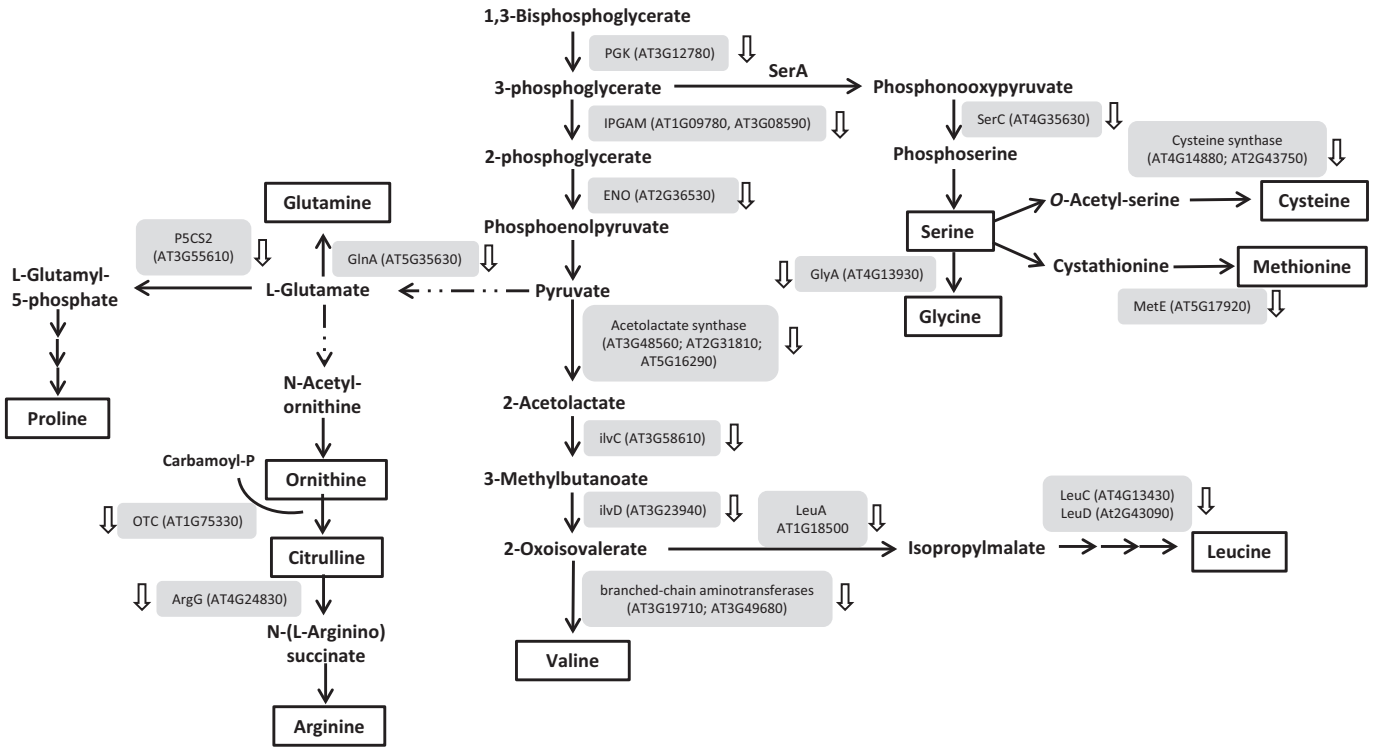

Fig. 3. Impact of nitrogen starvation on major amino acid biosynthesis pathways. Many enzymes involved in amino acid biosynthesis were identified with reduced abundances. ⇩ indicates decreased protein abundances. Dotted arrows represent multiple reaction steps. ArgG: argininosuccinate synthase G; ENO: enolase; GlnA: glutamine synthetase A; GlyA: glycine synthetase A; ilvC: ketol-acid reductoisomerase C; ilvD: Dihydroxy-acid dehydratase; IPGAM: 2,3-bisphosphoglycerate-independent phosphoglycerate mutase; LeuA: leucine synthase A; LeuC: 3-isoprppylmalate dehydratase large subunit; LeuD:3-isoprppylmalate dehydratase small subunit; MetE: methionine synthase E; OTC: ornithine carbamoyltransferase; P5CS2: delta 1-pyrroline-5-carboxylate synthase 2; PGK: phosphoglycerate kinase; SerC:serine synthase C.

GRF6 is translocated to the nucleus where it binds and destabilize the C-repeat-binding factor proteins required for cold acclimation [45]. Here, our work strongly suggests a positive regulatory role of GRF6 in nitrogen stress response. The precise targets of GRF6 and the associated phosphorylation events will require further investigations.

4. Materials and methods

4.1. Plant materials and growth conditions

Arabidopsis (*Arabidopsis thaliana*) wild-type (Col-0) was used in the proteomics investigation. Seeds were surface-sterilized, placed in the dark at 4 °C for two days, and then germinated on MS agar (Sigma) plates containing 1.5% sucrose (*w/v*). The plates were kept in a tissue culture room with a light/dark cycle of 16/8 h at 23 °C. After 7 days, 40 seedlings (one biological replicate) were transplanted to one well of a 12-well microplate (well diameter 22 mm, Brand: IWAKI, Product code: 3815-012). These 40 seedlings were treated as one biological replicate. The seedlings were cultured on 2 mL MS or MS-N (without nitrogen sources) liquid medium (adjusted to pH 5.6 by KOH) with 1.5% sucrose for 48 h under static condition (fresh medium was used after 24 h). Finally, the four biological replicates of the seedling samples were collected and frozen in liquid nitrogen. Ammonium, nitrate and chlorophyll contents were determined using commercial detection kits (Solarbio Cat#BC1500 and Cat#BC1520 Cat#BC0990).

4.2. Protein and Peptide Preparation

Approximately 1 g of Arabidopsis seedlings was ground in a mortar with liquid nitrogen. The tissues were homogenized by the 10× volume of solvent (10% trichloroacetic acid (TCA)/acetone) and centrifuged at 16000*g* at 4 °C for 5 min. The pellets were further washed with 10× volume of solvent (80% methanol/0.1 M ammonium acetate), and then further washed with 10× volume of 80% acetone. After centrifugation, the supernatants were removed, and the pellets were dissolved into 8 ml of SDT buffer (4% SDS, 0.1 M DTT and 0.1 M MOPS/HCl, pH 8.0). Afterwards, the homogenized samples were incubated at 95 °C for 10 min and cooled immediately on ice for 5 min. Clear supernatants were obtained after centrifugation twice, followed by addition of 4× volume of chilled 80% acetone for overnight protein precipitation at −20 °C. Finally, the protein pellets were dissolved in the 1–2 ml urea buffer (6 M urea in 200 mM MOPS-Cl/4 mM $CaCl_2$, pH 8.0). Protein concentration was determined using the Pierce™ BCA Protein Assay Kit (Thermo Scientific, USA) with bovine serum albumin as a standard for quantification.

Each protein sample (100 μg) was reduced by 10 mM dithiothreitol at 50 °C for 40 min and alkylated by 40 mM iodoacetamide at room temperature in darkness for 30 min. Afterwards, each sample was diluted into a final urea concentration below 2 M and then trypsin-digested overnight at 37 °C (enzyme/protein, 1:50 *w*/w). Peptides were generated by specific trypsin cleavage at the C-terminal at the arginine and lysine sites of proteins. The acquired peptides were acidified by 10% TCA and desalted using SepPak C18 cartridges (Waters). Finally, the desalted peptide samples were dried in a speed-vacuum concentrator and stored at −80 °C or directly dissolved in 0.1% formic acid for LC-MS/MS analysis.

4.3. SWATH-MS analysis

Peptides samples were analyzed by the Triple TOF 5600 mass spectrometer (SCIEX, USA) coupled with the Eksigent NanoLC-2D plus system. In the Trap-Elute mode, each sample (2 μg) was placed into a

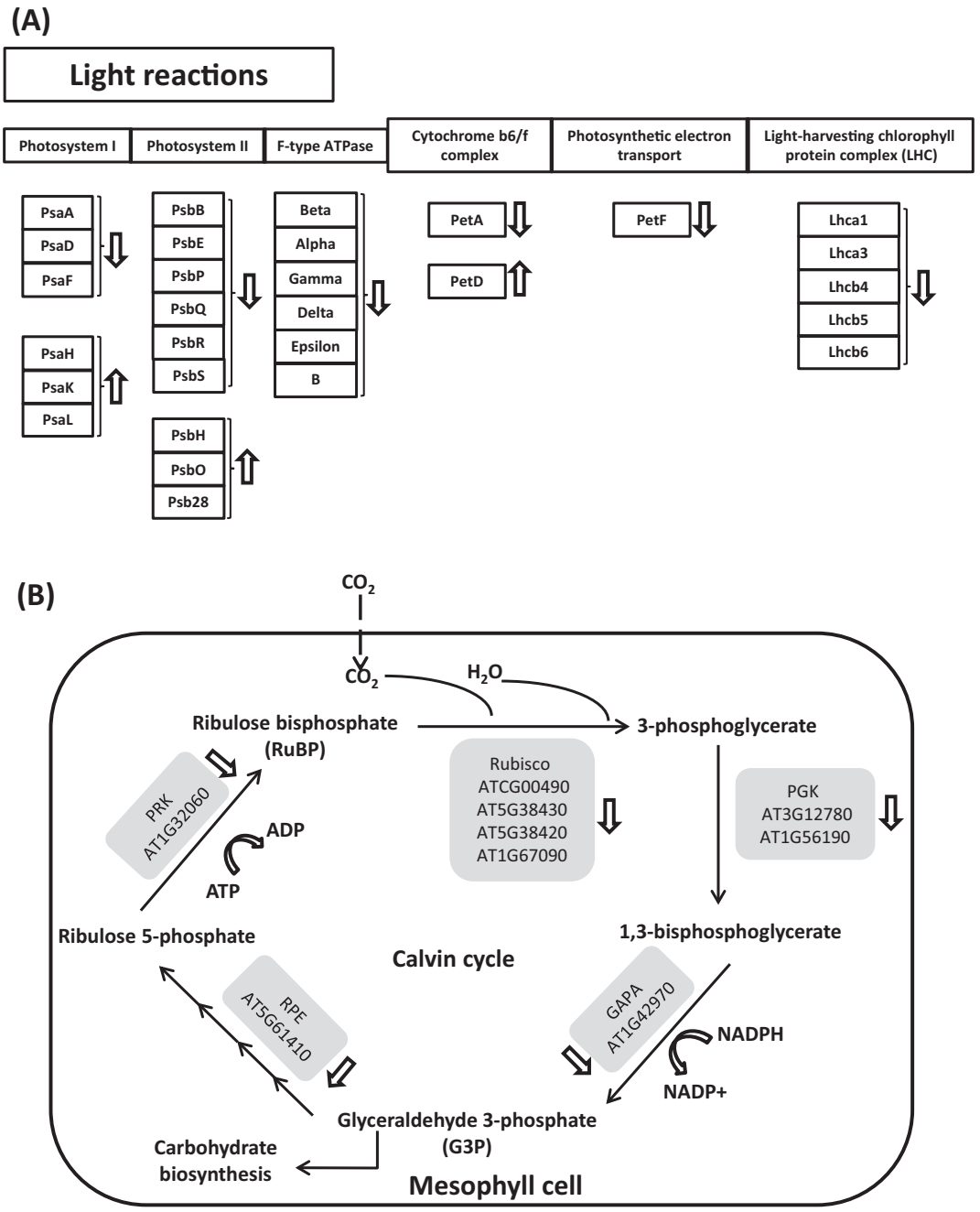

Fig. 4. Impact of nitrogen starvation on photosynthesis. (A). Reduced abundances of many proteins in different light reaction complexes were detected. Several proteins in photosystems I and II showed increased abundances (B). A number of enzymes involved in the CO_2 assimilation pathway were down-regulated. ⇩ and ⇧ indicate decreased and increased protein abundances, respectively. GAPA: glyceraldehyde-3-phosphate dehydrogenase A; PGK: phosphoglycerate kinase; PRK: phosphoribulokinase; RPE: ribulose-5-phosphate-3-epimerase; Rubisco: Ribulose-1,5-bisphosphate carboxylase/oxygenase.

nanaoFlexcHiPLC trap (3 μm, ChromXP C18CL, 120 Å, 0.5 mm × 200 μm) in 95% solvent A (water with 0.1% formic acid) and 5% solvent B (acetonitrile with 0.1% formic acid) at a steady flow rate of 500 nL/min for 15 min, then separated through a linear gradient from 5% to 35% of solvent B at 300 nL/min for 120 min. Positive ion mode with an ion spray voltage of 2300 V was used in the mass spectrometer. A spectral ion library based on SWATH-MS was first generated using data-dependent acquisition (DDA). In the DDA mode, the complete MS1 spectra were collected by a survey scan of 250 ms in the range of 350–1250 *m/z*. The top 40 precursor ions were selected for further MS2 fragmentation in the collision cell using rolling collision energy based on their m/z and charge state. MS/MS spectra were acquired in the range of 100–1800 m/z. In the SWATH analysis, the same peptide samples were analyzed by the cyclic data-independent acquisition (DIA) mode using similar methods as described above. Precursor ions in the range of 400–1250 Da were collected for further fragmentation. All DDA data files were used to generate a reference spectral library by searching against the UniProt Swiss-Prot *Arabidopsis thaliana* protein database (28797 proteins, July 2015 release) using the ProteinPilot 4.5 software (Sciex). The parameters included digestion, alkylation, and biological modification. A false discovery rate of < 1% was accepted as the criteria for the peptide assignments and protein identification. Subsequently, the DIA data and spectral library were loaded into PeakView v.1.2 software (Sciex) under restricted criteria and settings: eight peptides, six transitions, 99% peptide confidence and ion library mass tolerance (50 ppm). The output of quantified proteins

(A)

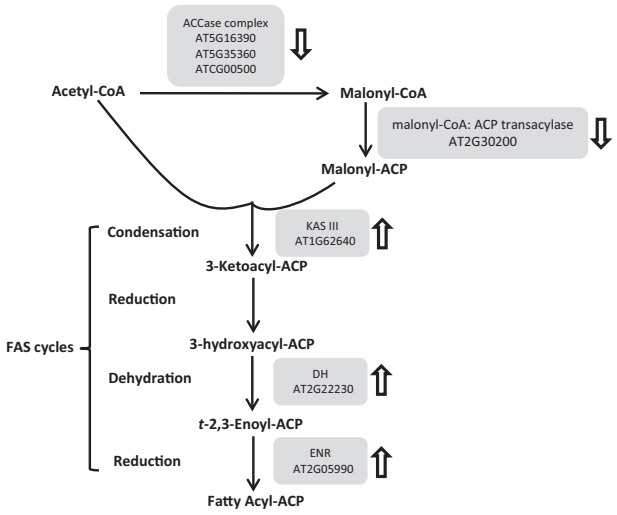

(B)

Lipid profiling (% of total phospholipids) of Arabidopsis seedlings under nitrogen deprivation

Lipid class	MS	MS-N
Digalactosyldiacylglycerol	13.22 ± 0.43	11.92 ± 1.65
Monogalactosyldiacylglycerol	58.90 ± 8.76	60.24 ± 11.98
Phosphatidic acid	0.52 ± 0.095	0.58 ± 0.052
Phosphatidylglycerol	6.47 ± 0.51	6.12 ± 0.64
Phosphatidylinositol	5.42 ± 0.44	5.18 ± 0.32
Phosphatidylserine	0.43 ± 0.081	0.24 ± 0.042*
Phosphatidylcholine (PC)	9.99 ± 0.35	11.58 ± 0.69*
Phosphatidyletanolamine (PE)	4.88 ± 0.15	3.99 ± 0.16*
LysoPC	0.053 ± 0.007	0.057 ± 0.007
LysoPE	0.076 ± 0.006	0.068 ± 0.005
LysoPG	0.010 ± 0.0007	0.011 ± 0.0006
PC/PE	2.047 ± 0.11	2.902 ± 0.13**

Fig. 5. Impact of nitrogen starvation on lipid metabolism and phospholipid composition following nitrogen deprivation. (A). A number of enzymes involved in fatty acid biosynthesis showed significant changes in protein abundances. ⇩ and ⇧ indicate decreased and increased protein abundances, respectively. ACCase, Acetyl-CoA carboxylase; DH, 3-hydroxyacyl-ACP dehydratase; ENR, enoyl-ACP reductase; FAS, fatty acid synthase; KAS III, 3-ketoacyl-ACP synthase III. (B). Phospholipid profiling of Arabidopsis seedlings. Seven-day-old Arabidopsis seedlings were grown on MS or MS-N liquid medium for 48 h. Data are averages of 4 biological replicates per treatment. Error bars represent SE ($n = 4$), *P < 0.05; **P < 0.01 by Student's *t*-test.

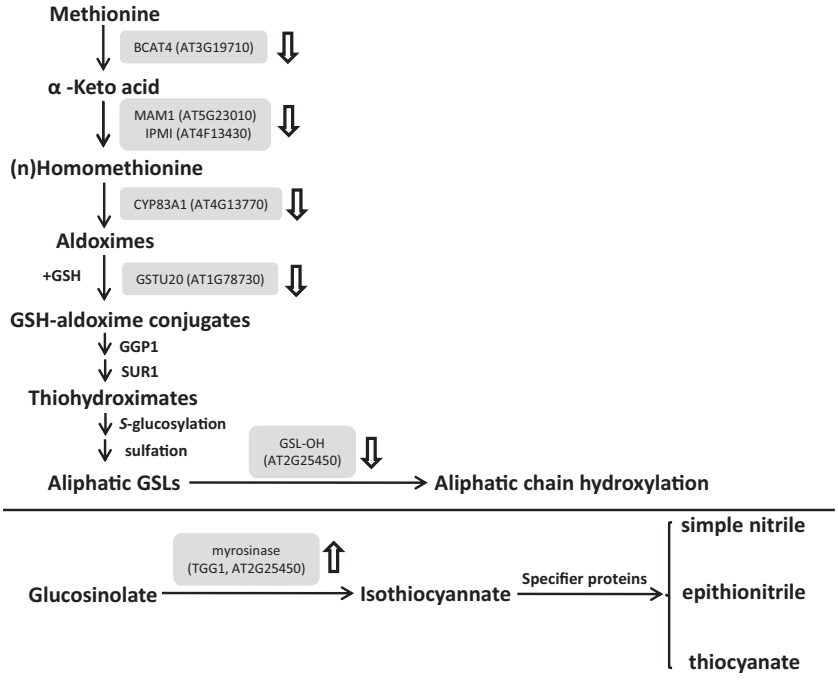

Fig. 6. Impact of nitrogen starvation on glucosinolate metabolism Biosynthesis of methionine-derived glucosinolates (GSLs) and the degradation pathway. Several enzymes involved in the biosynthesis of aliphatic GSLs showed decreased protein abundances while the myrosinase TGG1 which participates in GSL degradation showed increased protein abundances. ⇩ and ⇧ indicate decreased and increased protein abundances, respectively. BCAT4: branched-chain aminotransferase 4; CYP83A1: cytochrome P450 83A1; GGP1: gamma-glutamyl peptidase; GSH: glutathione; GSL-OH: GSL hydroxylase; GSTU20: glutathione S-transferase TAU20; IPMI: isopropylmalate isomerase; MAM1: methylthioalkylmalate synthase 1; SUR1: S-alkyl-thiohydroximate lyase 1.

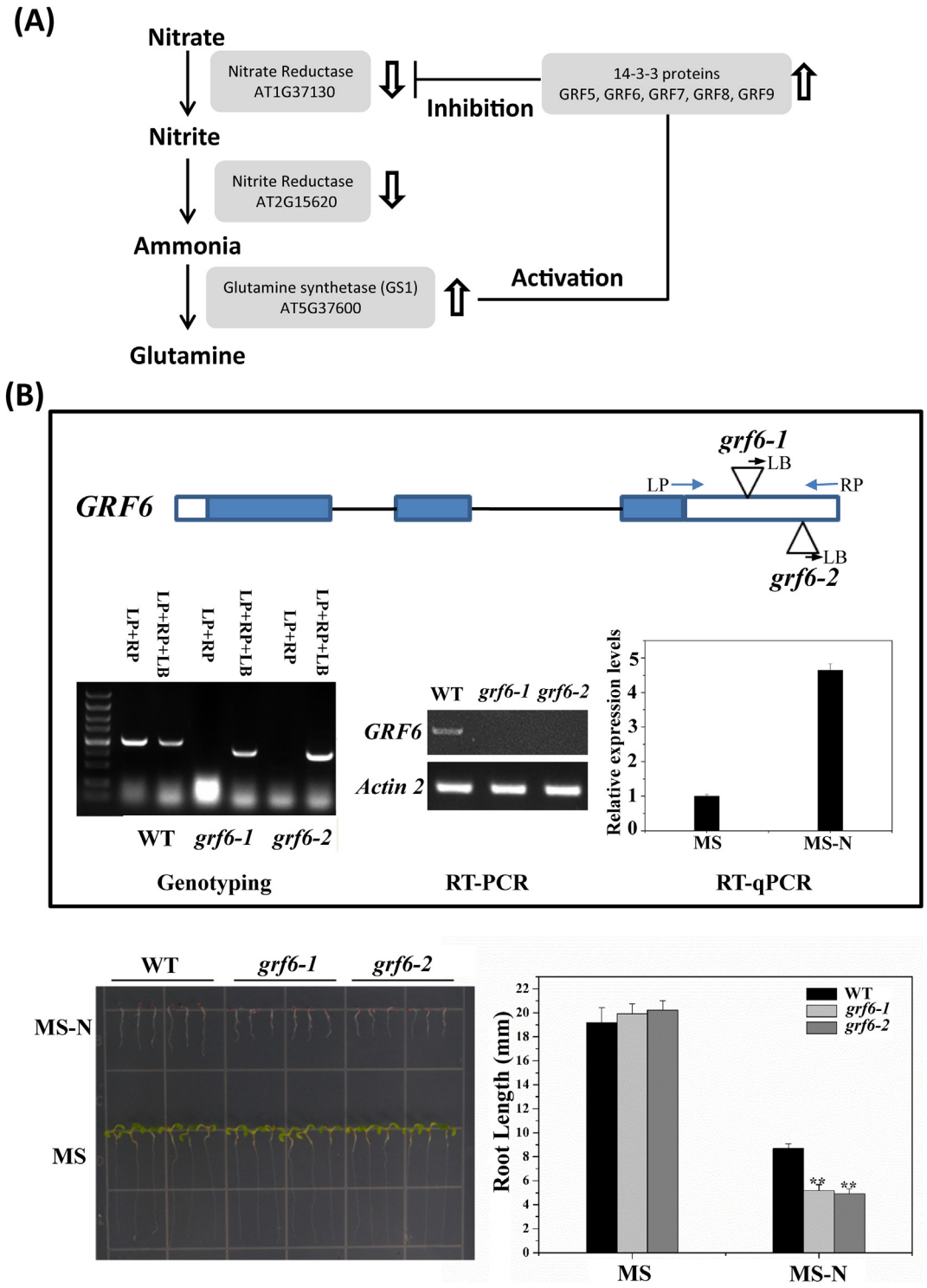

Fig. 7. Potential participation of 14–3-3 proteins in regulating nitrogen stress responses in Arabidopsis (A). Several 14–3-3 proteins known to inhibit nitrate reductase and activate cytosolic glutamine synthetase 1 activity showed increased abundances upon nitrogen starvation. ⇩ and ⇧ indicate decreased and increased protein abundances, respectively. (B). Analysis of two Arabidopsis *grf6* T-DNA insertion mutants. Representative PCR genotyping results are shown. *GRF6* is not expressed in the mutants (RT-PCR data) and is strongly inducible in nitrogen-starved wild-type (WT) seedlings (RT-qPCR data). Both mutant lines showed enhanced root inhibition upon nitrogen starvation. Error bars represent SE (n = 30); *P < 0.05; **P < 0.01 by Student's t-test.

and corresponding peptides by the MarkerView (Sciex) generated three quantitative files including the extracted peak area for individual fragment ions, the sum of the fragment ion areas for each peptide and the sum of peptide areas for each protein. The exported raw peak intensity data of proteins were normalized and analyzed using z-transformation as described previously [46, 47]. The raw data files have been submitted into the PRIDE PRoteomics IDEntifications (PRIDE) database with the accession number PXD007190.

4.4. Nitrogen starvation-induced root inhibition assay

Seeds of Arabidopsis WT and *grf6* T-DNA insertion mutants (*grf6–1*:

SALK_068774 and *grf6–2*: SALK_096602) were germinated on MS or MS-N agar (adjusted to pH 5.6 by KOH) containing 1.5% sucrose (*w/v*). The plates were kept at 4 °C in darkness for two days and then placed vertically in a tissue culture room with a light/dark cycle of 16/8 h at 23 °C. Root lengths were measured at day 10.

4.5. Analysis of phospholipids in Arabidopsis seedlings

Total plant lipids were extracted according to the method described previously [48]. Briefly, approximately 100 mg of seedlings were collected and immediately immersed in 3 ml isopropanol (preheated at 75 °C) with 0.01% butylated hydroxytoluene (BHT) for 15 min. Afterwards, 1.5 ml of chloroform and 0.6 ml of water were added, and the mixture was shaken at 150 g for 1 h. The lipid extracts were transferred to a 50-ml glass tube. Subsequently, 4 ml of chloroform/methanol (2:1) with 0.01% BHT was added into the initial seedling samples, followed by shaking for 30 min. This step was repeated 4–5 times until the seedlings became white. Each lipid extract was combined with 1 ml of 1 M KCl, centrifuged, and the upper aqueous phase was discarded. After adding 2 ml of water, pure lipid-extracts were obtained by centrifugation. Finally, the lipid extracts collected in the glass tubes were filled with nitrogen gas and stored at −80 °C. The extracted seedlings were further incubated at 105 °C overnight for dry weight determination. Subsequently, the profiles of membrane lipids in the samples were measured by automated electrospray ionization-tandem mass spectrometry and data analysis was performed essentially as described by Xie et al. [27].

4.6. Gene expression analysis

Total RNA was extracted from approximately 30 Arabidopsis seedlings using the Trizol reagent (Invitrogen). Subsequently, 5 μg RNA was reversed transcribed by M-MLV reverse transcriptase (Promega) for cDNA synthesis. PCR amplification was programmed as follows: pre-incubation (95 °C for 5 min), followed by 27 cycles of 95 °C for 30 s; 55 °C for 45 s; 72 °C for 45 s, and finalized by an extension step at 72 °C for 7 min. SYBR Green Mix (Applied Biosystems) was used for quantitative PCR experiments which were performed in the StepOne Plus real-time PCR system using the following program: pre-incubation (95 °C C for 10 min), followed by 40 cycles of 95 °C for 15 s and 56 °C for 1 min. Relative gene expression levels were determined by the comparative CT method [49] using *Actin 2* (At3g18780) as a reference. Primer information used in gene expression analysis described above is listed in Table S4.

Supplementary data to this article can be found online at https://doi.org/10.1016/j.jprot.2018.07.014.

Acknowledgements

The work was supported by the HKU small project funding (project numbers 201309176152 and 201209176039), the National Natural Science Foundation of China (NSFC31701341), the China Postdoctoral Science Foundation (2017M622801), Hong Kong Research Grant Council (AoE/M- 05/12, AoE/M-403/16, CUHK 474313, 14122415), the NJFU project funding (GXL2018005) and Shenzhen Overseas Talents Innovation and Entrepreneurship Funding Scheme (The Peacock Scheme, KQTD201101).

References

[1] C. Masclaux-Daubresse, F. Daniel-Vedele, J. Dechorgnat, F. Chardon, L. Gaufichon, A. Suzuki, Nitrogen uptake, assimilation and remobilization in plants: challenges for sustainable and productive agriculture, Ann. Bot. 105 (7) (2010) 1141–1157.
[2] A.V. Barker, G.M. Bryson, Nitrogen, in: A.V. Barker, D.J. Pilbeam (Eds.), Handbook of Plant Nutrition, CRC Press, Boca Raton, 2006, pp. 21–50.
[3] H.M. Lam, K. Coschigano, I. Oliveira, R. Melo-Oliveira, G. Coruzzi, The molecular-genetics of nitrogen assimilation into amino acids in higher plants, Annu. Rev. Plant Biol. 47 (1) (1996) 569–593.
[4] A.J. Miller, X. Fan, M. Orsel, S.J. Smith, D.M. Wells, Nitrate transport and signalling, J. Exp. Bot. 58 (9) (2007) 2297–2306.
[5] D. Fowler, M. Coyle, U. Skiba, M.A. Sutton, J.N. Cape, S. Reis, L.J. Sheppard, A. Jenkins, B. Grizzetti, J.N. Galloway, The global nitrogen cycle in the twenty-first century, Philos. T. R. Soc. B 368 (1621) (2013) 20130165.
[6] L.E. Jackson, M. Burger, T.R. Cavagnaro, Roots, nitrogen transformations, and ecosystem services, Annu. Rev. Plant Biol. 59 (2008) 341–363.
[7] T. Garnett, V. Conn, B.N. Kaiser, Root based approaches to improving nitrogen use efficiency in plants, Plant Cell Environ. 32 (9) (2009) 1272–1283.
[8] G. Xu, X. Fan, A.J. Miller, Plant nitrogen assimilation and use efficiency, Annu. Rev. Plant Biol. 63 (2012) 153–182.
[9] D. Loqué, L. Yuan, S. Kojima, A. Gojon, J. Wirth, S. Gazzarrini, K. Ishiyama, H. Takahashi, N. Von Wirén, Additive contribution of AMT1;1 and AMT1;3 to high-affinity ammonium uptake across the plasma membrane of nitrogen-deficient Arabidopsis roots, Plant J. 48 (4) (2006) 522–534.
[10] L. Yuan, D. Loqué, S. Kojima, S. Rauch, K. Ishiyama, E. Inoue, H. Takahashi, N. von Wirén, The organization of high-affinity ammonium uptake in Arabidopsis roots depends on the spatial arrangement and biochemical properties of AMT1-type transporters, Plant Cell 19 (8) (2007) 2636–2652.
[11] L. Yuan, D. Loqué, F. Ye, W.B. Frommer, N. von Wirén, Nitrogen-dependent post-transcriptional regulation of the ammonium transporter AtAMT1;1, Plant Physiol. 143 (2) (2007) 732–744.
[12] A. Krapp, L.C. David, C. Chardin, T. Girin, A. Marmagne, A.-S. Leprince, S. Chaillou, S. Ferrario-Méry, C. Meyer, F. Daniel-Vedele, Nitrate transport and signalling in Arabidopsis, J. Exp. Bot. 65 (3) (2014) 789–798.
[13] S. Léran, K. Varala, J.-C. Boyer, M. Chiurazzi, N. Crawford, F. Daniel-Vedele, L. David, R. Dickstein, E. Fernandez, B. Forde, A unified nomenclature of nitrate transporter 1/peptide transporter family members in plants, Trends Plant Sci. 19 (1) (2014) 5–9.
[14] T. Kiba, A. Krapp, Plant nitrogen acquisition under low availability: regulation of uptake and root architecture, Plant Cell Physiol. 57 (4) (2016) 707–714.
[15] C.H. Ho, S.H. Lin, H.C. Hu, Y.F. Tsay, CHL1 functions as a nitrate sensor in plants, Cell 138 (6) (2009) 1184–1194.
[16] W.R. Scheible, R. Morcuende, T. Czechowski, C. Fritz, D. Osuna, N. Palacios-Rojas, D. Schindelasch, O. Thimm, M.K. Udvardi, M. Stitt, Genome-wide reprogramming of primary and secondary metabolism, protein synthesis, cellular growth processes, and the regulatory infrastructure of Arabidopsis in response to nitrogen, Plant Physiol. 136 (1) (2004) 2483–2499.
[17] R. Wang, M. Okamoto, X. Xing, N.M. Crawford, Microarray analysis of the nitrate response in Arabidopsis roots and shoots reveals over 1,000 rapidly responding genes and new linkages to glucose, trehalose-6-phosphate, iron, and sulfate metabolism, Plant Physiol. 132 (2) (2003) 556–567.
[18] N. Bahrman, J. Le Gouis, L. Negroni, L. Amilhat, P. Leroy, A.L. Lainé, O. Jaminon, Differential protein expression assessed by two-dimensional gel electrophoresis for two wheat varieties grown at four nitrogen levels, Proteomics 4 (3) (2004) 709–719.
[19] A.L. Møller, P. Pedas, B. Andersen, B. Svensson, J.K. Schjoerring, C. Finnie, Responses of barley root and shoot proteomes to long-term nitrogen deficiency, short-term nitrogen starvation and ammonium, Plant Cell Environ. 34 (12) (2011) 2024–2037.
[20] S. Dutt, J. Parkash, R. Mehra, N. Sharma, B. Singh, P. Raigond, A. Joshi, S. Chopra, B. Singh, Translation initiation in plants: roles and implications beyond protein synthesis, Biol. Plant. 59 (3) (2015) 401–412.
[21] C. Pascuan, R. Frare, K. Alleva, N.D. Ayub, G. Soto, mRNA biogenesis-related helicase eIF4AIII from Arabidopsis thaliana is an important factor for abiotic stress adaptation, Plant Cell Rep. 35 (5) (2016) 1205–1208.
[22] A.D. Lellis, K.D. Kasschau, S.A. Whitham, J.C. Carrington, Loss-of-susceptibility mutants of Arabidopsis thaliana reveal an sssential role for eIF(iso)4E during *Potyvirus* infection, Curr. Biol. 12 (12) (2002) 1046–1051.
[23] M. Sato, K. Nakahara, M. Yoshii, M. Ishikawa, I. Uyeda, Selective involvement of members of the eukaryotic initiation factor 4E family in the infection of *Arabidopsis thaliana* by potyviruses, FEBS Lett. 579 (5) (2005) 1167–1171.
[24] Y. Chen, E.H. Murchie, S. Hubbart, P. Horton, S. Peng, Effects of season-dependent irradiance levels and nitrogen-deficiency on photosynthesis and photoinhibition in field-grown rice (Oryza sativa), Physiol. Plant. 117 (3) (2003) 343–351.
[25] S. Doncheva, V. Vassileva, G. Ignatov, S. Pandev, R. Dris, R. Niskanen, Influence of nitrogen deficiency on photosynthesis and chloroplast ultrastructure of pepper plants, Agr. Food Sci. Finland 10 (2001) 59–64.
[26] X. Wang, Lipid signaling, Curr. Opin. Plant Biol. 7 (3) (2004) 329–336.
[27] L.J. Xie, Q.F. Chen, M.X. Chen, L.J. Yu, L. Huang, L. Chen, F.Z. Wang, F.N. Xia, T.R. Zhu, J.X. Wu, Unsaturation of very-long-chain ceramides protects plant from hypoxia-induced damages by modulating ethylene signaling in Arabidopsis, PLoS Genet. 11 (3) (2015) e1005143.
[28] R.G. Upchurch, Fatty acid unsaturation, mobilization, and regulation in the response of plants to stress, Biotechnol. Lett. 30 (6) (2008) 967–977.
[29] A.P. Brown, A.R. Slabas, J.B. Rafferty, Fatty acid biosynthesis in plants-metabolic pathways, structure and organization, in: H. Wada, N. Murata (Eds.), Lipids in Photosynthesis. Advances in Photosynthesis and Respiration, 30 Springer, Dordrecht, 2009, pp. 11–34.
[30] D.A. Los, N. Murata, Membrane fluidity and its roles in the perception of environmental signals, BBA-Biomembranes 1666 (1) (2004) 142–157.
[31] B.L. Örvar, V. Sangwan, F. Omann, R.S. Dhindsa, Early steps in cold sensing by plant cells: the role of actin cytoskeleton and membrane fluidity, Plant J. 23 (6) (2000) 785–794.
[32] V.A. Fajardo, L. McMeekin, P.J. Leblanc, Influence of phospholipid species on

membrane fluidity: a meta-analysis for a novel phospholipid fluidity index, J. Membr. Biol. 244 (2) (2011) 97–103.
[33] J.A. Killian, B. de Kruijff, Nonbilayer lipids affect peripheral and integral membrane proteins via changes in the lateral pressure profile, BBA-Biomembranes 1666 (1) (2004) 275–288.
[34] Y.Z. Chen, Q.Y. Pang, Y. He, N. Zhu, I. Branstrom, X.F. Yan, S. Chen, Proteomics and metabolomics of Arabidopsis responses to perturbation of glucosinolate biosynthesis, Mol. Plant 5 (5) (2012) 1138–1150.
[35] S. Chen, E. Andreasson, Update on glucosinolate metabolism and transport, Plant Physiol. Biochem. 39 (9) (2001) 743–758.
[36] D. Marino, I. Ariz, B. Lasa, E. Santamaría, J. Fernández-Irigoyen, C. González-Murua, P.M.A. Tejo, Quantitative proteomics reveals the importance of nitrogen source to control glucosinolate metabolism in *Arabidopsis thaliana* and *Brassica oleracea*, J. Exp. Bot. 67 (11) (2016) 3313–3323.
[37] A.M. Bones, J.T. Rossiter, The myrosinase-glucosinolate system, its organisation and biochemistry, Physiol. Plant. 97 (1) (1996) 194–208.
[38] U. Wittstock, M. Burow, Glucosinolate breakdown in Arabidopsis: mechanism, regulation and biological significance, The Arabidopsis Book, vol. 8, 2010 (e0134).
[39] K. Falk, J. Tokuhisa, J. Gershenzon, The effect of sulfur nutrition on plant glucosinolate content: physiology and molecular mechanisms, Plant Biol. 9 (5) (2007) 573–581.
[40] M. Bachmann, J.L. Huber, G.S. Athwal, K. Wu, R.J. Ferl, S.C. Huber, 14-3-3 proteins associate with the regulatory phosphorylation site of spinach leaf nitrate reductase in an isoform-specific manner and reduce dephosphorylation of Ser-543 by endogenous protein phosphatases, FEBS Lett. 398 (1) (1996) 26–30.
[41] J. Finnemann, J.K. Schjoerring, Post-translational regulation of cytosolic glutamine synthetase by reversible phosphorylation and 14-3-3 protein interaction, Plant J. 24 (2) (2000) 171–181.
[42] J. Yan, C. He, J. Wang, Z. Mao, S.A. Holaday, R.D. Allen, H. Zhang, Overexpression of the Arabidopsis 14-3-3 protein GF14 lambda in cotton leads to a "stay-green" phenotype and improves stress tolerance under moderate drought conditions, Plant Cell Physiol. 45 (8) (2004) 1007–1014.
[43] X.H. Yang, W.M. Wang, M. Coleman, U. Orgil, J.Y. Feng, X.F. Ma, R. Ferl, J.G. Turner, S.Y. Xiao, Arabidopsis 14-3-3 lambda is a positive regulator of RPW8-mediated disease resistance, Plant J. 60 (3) (2009) 539–550.
[44] A. Latz, N. Mehlmer, S. Zapf, T.D. Mueller, B. Wurzinger, B. Pfister, E. Csaszar, R. Hedrich, M. Teige, D. Becker, Salt stress triggers phosphorylation of the Arabidopsis vacuolar K+ channel TPK1 by calcium-dependent protein kinases (CDPKs), Mol. Plant 6 (4) (2013) 1274–1289.
[45] Z. Liu, Y. Jia, Y. Ding, Y. Shi, Z. Li, Y. Guo, Z. Gong, S. Yang, Plasma Membrane CRPK1-Mediated Phosphorylation of 14-3-3 Proteins induces their nuclear import to fine-tune CBF signaling during cold response, Mol. Cell 66 (1) (2017) 117–128.
[46] N.A. Haverland, H.S. Fox, P. Ciborowski, Quantitative proteomics by SWATH-MS reveals altered expression of nucleic acid binding and regulatory proteins in HIV-1-infected macrophages, J. Proteome Res. 13 (4) (2014) 2109–2119.
[47] C. Cheadle, M.P. Vawter, W.J. Freed, K.G. Becker, Analysis of microarray data using Z score transformation, J. Mol. Diagn. 5 (2) (2003) 73–81.
[48] R. Welti, W. Li, M. Li, Y. Sang, H. Biesiada, H.E. Zhou, C. Rajashekar, T.D. Williams, X. Wang, Profiling membrane lipids in plant stress responses role of phospholipase Dα in freezing-induced lipid changes in Arabidopsis, J. Biol. Chem. 277 (35) (2002) 31994–32002.
[49] T.D. Schmittgen, K.J. Livak, Analyzing real-time PCR data by the comparative CT method, Nat. Protoc. 3 (6) (2008) 1101–1108.